

# Exploration of the Molecular Characteristics of the Tumor–Immune Interaction and Analysis of Immune Implication of CXCR4 in Gastric Cancer

**Fang Wen**

Nanjing University of Chinese Medicine

**Xiaona Lu**

Nanjing University of Chinese Medicine

**Wenjie Huang**

Nanjing University of Chinese Medicine

**Xiaoxue Chen**

Nanjing University of Chinese Medicine

**Shuai Ruan**

Nanjing University of Chinese Medicine

**SuPing Gu**

Nanjing University of Chinese Medicine

**Yulan Wang**

Nanjing University of Chinese Medicine

**Ye Li**

Nanjing University of Chinese Medicine

**Jiatong Liu**

Nanjing University of Chinese Medicine

**Shenlin Liu**

Nanjing University of Chinese Medicine

**Peng Shu** (✉ [shupengsp@njucm.edu.cn](mailto:shupengsp@njucm.edu.cn))

Nanjing University of Chinese Medicine <https://orcid.org/0000-0001-5611-5198>

---

## Primary research

**Keywords:** Tumor microenvironment, gastric cancer, immune cells, CXCR4, prognosis

**Posted Date:** July 6th, 2021

**DOI:** <https://doi.org/10.21203/rs.3.rs-570615/v1>

**License:**  This work is licensed under a Creative Commons Attribution 4.0 International License.

[Read Full License](#)

---

# Abstract

**Background:**Gastric cancer (GC) is rated as one of the most commonly diagnosed cancers and the leading cause of cancer-related deaths in the world. Despite the emergence of a combination of surgery, surveillance endoscopy, chemotherapy, radiotherapy, and various novel treatment strategies in recent years, the prognosis for patients with gastric cancer is far from optimistic due to its predisposition to invasion or metastasis and low rate of early diagnosis. GC exists in a complex tumor–immune microenvironment. Immune cell infiltration and tumor–immune molecules play a key role in tumor development and are closely related to the prognosis of patients. Therefore, understanding the cellular composition and function of TME is essential to grasp the tumor progression of GC, and is helpful to find molecular markers with the prognostic value that affect the immune response of GC patients.

**Methods:**In this study, we performed multiple machine learning algorithms to identify immunophenotypes and immunological characteristics in GC patient's data from the TCGA database and identified immune-related genes involved in the GC-immune interaction. In addition, we used R software and online databases to assess the status of lymphocytes and clarified the association between the hub gene and GC immunity, as well as the signaling pathways that regulate the immune response mediated by the hub gene.

**Results:**In this study, we found a close linkage between CXCR4 and the immunity of GC. The CXCR4 gene expression was associated with immune cell infiltration levels and immunomodulators. We established an immune gene model for GC using CXCR4-associated immunomodulators. The risk scores derived from the gene signatures were significantly associated with survival in GC. And, our results demonstrated that the risk scores derived from CXCR4-associated immunomodulators could distinguish risk groups defined by differential expression of a set of signature genes.

**Conclusions:** Our findings provided evidence of CXCR4's implication in tumor immunity, suggesting that CXCR4 may be a potential prognostic biomarker and immunotherapeutic target for GC. The prognostic immune markers from CXCR4-associated immunomodulators could independently predict the overall survival of GC. The prognostic immune model using CXCR4-associated immunomodulators contribute to the individualization of the clinical treatment strategy to improve the survival chances of patients.

## Introduction

Gastric cancer (GC) is rated as one of the most commonly diagnosed cancers and the leading cause of cancer-related deaths in the world[1]. Despite the emergence of a combination of surgery, surveillance endoscopy, chemotherapy, radiotherapy and various novel treatment strategies in recent years, the prognosis for patients with gastric cancer is far from optimistic due to its predisposition to invasion or metastasis and low rate of early diagnosis[2–4]. The tumor microenvironment (TME) is the environment where tumor cells are located, which can promote tumor growth and metastasis and immune escape[5, 6]. In addition to tumor cells, TME also includes endothelial cells, immune cells, mesenchymal cells,

extracellular matrix (ECM) molecules, and inflammatory mediators[7, 8]. Studies have shown that changes in the content of immune cells and stromal cells in TME play an important role in tumor diagnosis and prognosis[9]. In the TME, tumor cells interact closely with stromal cells, immune cells and ECM. Through complex mechanisms, these communications support tumor growth, metastatic spread, and immune escape. Immunotherapy based on immunological checkpoint inhibitors or targeted drugs has been emerging as a promising alternative treatment for some cancer patients[10, 11]. However, only a small percentage of cancer patients benefit from immunotherapy. Immune escape has been proven to be a sign of cancers that rely on the immune microenvironment, and it is also one of the important reasons for the failure of immunotherapy in tumor patients[12, 13]. The proportional imbalance between regulatory cells and effector cells in tumor-related microenvironment is the main mechanism to encourage immune escape. Some clinical trials have shown that tumor-infiltrating leukocytes are associated with clinical efficacy and cancer prognosis[14–17]. Therefore, understanding the cellular composition and function of TME is essential to grasp the tumor progression of GC, and is helpful to find molecular markers with the prognostic value that affect the immune response of GC patients.

In this study, we systematically explored the GC immune interaction associated molecular characteristics, which preliminarily revealed the complicated biological functions and immunological processes involved and the regulatory networks of these molecules. C-X-C motif chemokine receptor 4 (CXCR4), is a member of the C-X-C chemokine receptor family, which is associated with multiple types of cancer. CXCR4 gene is a promising therapeutic target in cancers, including hepatocellular carcinoma[18], gastrointestinal cancer[19], small cell lung cancer[20], breast cancer[21], and ovarian cancer[22]. Here we systematically evaluated the status of lymphocytes and clarified the association between CXCR4 and GC immunity, as well as the signaling pathways regulating the CXCR4-mediated immune response. Moreover, we constructed the prognostic immune model using CXCR4-associated immunomodulators to help the individualization of the clinical treatment strategy to improve the survival chances of patients.

## Methods

### 1. Data Collection

Transcriptome data and clinical data were downloaded from The Cancer Genome Atlas (TCGA, <https://portal.gdc.cancer.gov/>) database. The collation and extraction of data information used Perl scripts.

### 2. Survival analysis and related clinical parameters analysis of the tumor microenvironment

The R package "ESTIMATE" was used to score stromal cells and immune cells in TME. Use the R packages "survival" and "survminer" to combine the TME scores (Stromal score, Immune score, ESTIMATE score) with the survival data of the samples and analyze them. The samples with different immune activity were clustered according to immune score. Based on the median value of the TME scores, the samples were divided into high- and low-score groups, and the survival differences between the two

groups were analyzed. The R package "ggpubr" was used to analyze the difference between TME scores and clinical parameters and different immune activity groups.

### **3. Screening of differentially expressed genes and the hub gene**

The differentially expressed genes (DEGs) between high- and low- score groups of the stromal score and immune score were analyzed respectively. The filter condition was  $|\log_2(\text{fold change, FC})| > 1$  and false discovery rate (FDR)  $< 0.05$ . The DEGs in stromal cells were intersected with those in immune cells, and the intersecting DEGs were enriched and analyzed. The protein-protein interaction (PPI) network of the intersecting DEGs was constructed via the STRING database (<https://string-db.org/>) and Cytoscape software version 3.7.1(<https://cytoscape.org/>). The number of adjacent nodes of each gene in PPI was analyzed and the hub gene was obtained. Univariate Cox regression analysis was performed to screen prognostic-related genes. The prognosis-related hub gene (PRHG) was obtained by the intersection of the prognosis-related genes and hub genes.

## **4. Analysis Of The Prognostic-related Hub Gene**

The differences and pairing differences of PRHG between the normal group and tumor group were analyzed by using R packages "beeswarm" and "ggpubr" respectively. To further verify the expression of PRHG, the mRNA level was validated by the Gene Expression Profiling Interactive Analysis database (GEPIA, <http://gepia.cancer-pku.cn/>) and the TIMER database (<https://cistrome.shinyapps.io/timer/>). R packages "survival", "survminer" and "ggpubr" were used to analyze the overall survival time and clinical correlation of PRHG with different expression levels. Gene Set Enrichment Analysis (GSEA) v4.0.1 software (<https://www.gsea-msigdb.org/gsea/login.jsp>) was performed to reveal PRHG related biological pathways and mechanisms.  $P < 0.05$  was considered statistically significant.

### **5. The correlation analysis between PRHG and immune cells in TME**

The relative content of immune cells in each sample was calculated by the CIBERSORT algorithm (R Script v1.03), and the correlation between different immune cells was analyzed by R package "corrplot". Next, we analyzed the correlation between PRHG expression and immune cell infiltration in GC. The CIBERSORT R script obtained from the CIBERSORT website (<https://cibersort.stanford.edu/>) was used to analyze the relationship between the hub gene and immune grouping and different immune cells.

### **6. Construction of the immune prognosis model based on PRHG-related immunomodulators**

We searched the TISIDB database (<http://cis.hku.hk/TISIDB/>) for immunomodulators related to PRHG, including immunoinhibitor, immunostimulator, and major histocompatibility complex (MHC) molecule (Spearman correlation test,  $P < 0.05$ ).

A prognostic multiple immune gene model was constructed based on PRHG-related immunomodulators. We used univariate Cox analysis to initially identify potential immune genes. The expression values of

immune genes were weighted by the regression coefficient of the Cox regression model to calculate the risk score of every patient. Risk score= (Coefficient<sub>mRNA1</sub> × mRNA1 expression) + (Coefficient<sub>mRNA2</sub> × mRNA2 expression) + ... + (Coefficient<sub>mRNA<sub>n</sub></sub> × mRNA<sub>n</sub> expression). Kaplan-Meier survival curve was used to evaluate the association between the immune prognosis model and overall survival.

## 7. Independence Of The Immune Prognosis Model

Univariate and multivariate Cox regression analysis were performed to analyze the independent prognosis of GC patients with forwarding stepwise procedure,  $P < 0.05$  indicated statistical significance. The time-dependent receiver operating characteristic (ROC) curves were utilized to study the prognostic value of the risk score using the "SurvivalROC"[23] of R package. Nomogram[24] was constructed by including all independent prognostic factors to predict the survival of GC patients at 1 year, 3 years, and 5 years.

## 8. Statistical Analysis

R software (version 3.6.1, <https://cran.r-project.org/bin/windows/base/>) was applied to perform all statistical analyses. Wilcoxon test was suitable for comparison of data between two groups and Kruskal-Wallis test was performed for three or more groups. The survival data were analyzed by Kaplan-Meier curves and log-rank tests. Qualitative variables were compared by Pearson  $\chi^2$  test or Fisher's exact test. Spearman correlation test was used to analyze the correlation between immune cells. All comparisons in this study, a two-tailed  $p$ -value  $< 0.05$  was considered statistically significant.

## Results

### 1. Association with stromal score and immune score with survival analysis and clinical parameters

375 samples with GC and 32 normal samples were downloaded from the TCGA database. The stromal scores and immune scores of all samples were obtained by the ESTIMATE algorithm. And the score ranges were -1859.703 to 2072.280 and -1056.272 to 3124.198, respectively. What's more, the ESTIMATE score was -2471.016 to 4868.812.

To analyze the correlation between the stromal/immune/estimate scores and the overall survival of the samples, all samples were divided into high and low score groups. The Kaplan-Meier survival curve showed that the low score group of the stromal score has a higher 5-year survival rate than the high score group of the stromal score (Figure 1A). It suggested that the content of stromal cells in the GC microenvironment was related to the survival of patients. Survival rates were not significantly different in the high and low score groups of the immune/estimate scores (Figure 1B, C).

By exploring the potential relationship between the stromal/immune/estimate scores and the and clinical parameters, we observed that grade, stage, and tumor infiltration depth (T) had significant differences in scores (Figure 1D, E). In terms of the median value of stage, stage II, III, IV in the stromal and estimate median scores were higher than stage I, with

statistical significance. From the aspect of the median value of grade, grade 3 was higher than grade 2 in the stromal score, grade 3 was higher than grade 2 and grade 1 in the immune score, and grade 3 was higher than grade 1 in the estimate score, all with statistical significance. For the median value of tumor infiltration depth (T), T2, T3, and T4 were higher than T1 in the stromal/immune/estimate scores, with statistical significance. Taken together, the correlation analyses of stromal and immune scores with clinical parameters of GC revealed that both high stromal and immune scores were related to poor tumor differentiation and severe local invasion and that neither was significantly related to lymph nodes and distant metastasis, indicative of the greater influence of TME on primary tumor cells than metastasis.

## **2. The characteristics of the tumor microenvironment and immunophenotypes**

375 samples were analyzed using 29 immune gene sets according to the ssGSEA algorithm to evaluate the immune characteristics of GC patients. Based on the hierarchical clustering algorithm, the samples were clustered into three categories: 32 samples were clustered into cluster 1, 213 samples were clustered into cluster 2, and 128 samples were clustered into Cluster 3 (Figure 2A). As shown in Figure 2B, the immune characteristics of Cluster 1, Cluster 2 and Cluster 3 were compared—the immune characteristics of the three groups from high level to low level were: cluster 1 characteristics (Immunity High group) > cluster 2 characteristics (Immunity Medium group) > cluster 3 (Immunity Low group).

Next, according to the scores of the tumor microenvironment (TME) of each sample, the TME characteristics in the Immunity High/ Medium /Low groups were analyzed (Figure 2C). For the Immunity High group, StromalScore, ImmuneScore, EstimateScore, and TumorPurity were  $717.300 \pm 601.444$ ,  $2543.920 \pm 287.686$ ,  $3261.219 \pm 784.388$ , and  $0.465 \pm 0.101$ , respectively. The Immunity Low group had the opposite trend: StromalScore, ImmuneScore, EstimateScore, and TumorPurity were  $-478.587 \pm 674.297$ ,  $251.226 \pm 426.450$ ,  $-227.361 \pm 969.231$ , and  $0.833 \pm 0.076$ , respectively. The Immunity Medium group was somewhere between Immunity High group and Immunity Low group: StromalScore, ImmuneScore, EstimateScore, and TumorPurity were  $388.558 \pm 722.886$ ,  $1425.995 \pm 500.151$ ,  $1814.553 \pm 1072.298$ ,  $0.636 \pm 0.119$ , respectively.

The characteristics of the TME in the three groups were statistically significant differences (Figure 2E–G). In terms of tumor purity, the Immunity Low group had the highest level, while the Immunity High group had the lowest. Correspondingly, the Immunity High group had the highest infiltration degree of stromal cells and immune cells, and the lowest infiltration degree of stromal cells and immune cells in the Immunity Low group. All in all, with the decrease of tumor cell activity, the immune cell activity increased.

## **3. Identification and functional enrichment analysis of differentially expressed genes between high- and low-score groups**

To disclose the potential relationship between the stromal/immune scores and the gene expression profile of the GC samples, we explored the differential analysis of transcriptome data of GC patients (Figure 3A, B). As can be seen from the Venn diagram, there were 640 identical up-regulated genes and 120 identical down-regulated genes (Figure 3C, D). The volcano plot revealed the top 10 up-regulated genes and the top 10 down-regulated genes (Figure 3E).

We performed functional enrichment analysis on the obtained 760 differentially expressed genes (640 up-regulated genes and 120 down-regulated genes). Gene Ontology (GO) functions were mainly enriched in leukocyte proliferation—lymphocyte proliferation—mononuclear cell proliferation—regulation of lymphocyte activation—T cell activation—and lymphocyte differentiation (Figure 3F, G), while Kyoto Encyclopedia of Genes and Genomes (KEGG) pathways were mainly enriched in viral protein interaction with cytokine and cytokine receptor, staphylococcus aureus infection, hematopoietic cell lineage, chemokine signaling pathway, cytokine-cytokine receptor interaction, cell adhesion

molecules (CAMs), and phagosome (Figure 3H, I). These results suggest that differentially expressed genes are associated with immune function.

#### **4. Identification and verification of the prognostic-related hub gene**

We constructed a PPI network of genes with prognostic values using the STRING network to analyze the interrelationship between genes with prognostic values. In this PPI network, there were 188 nodes and 372 edges, with red nodes representing up-regulated genes and purple nodes representing down-regulated genes (Figure 4A). The hub genes in the PPI network were identified by analyzing the number of adjacent nodes of each gene. Figure 4B showed the top 30 hub genes from the PPI network. To obtain the prognostic-related genes, we performed a univariate COX analysis of 760 differentially expressed genes (Figure 4C). The result showed that the 26 genes related to prognosis were high-risk genes (hazard ratio,  $HR > 1$ ), unfortunately, indicating poor prognosis.

The intersection of PPI hub genes and prognostic-related genes was taken to obtain the hub prognostic gene (Figure 4D). Analyzing the expression of the CXCR4 gene in the samples, we found that CXCR4 was significantly different between the normal and tumor groups ( $P < 0.05$ ), it was down-regulated in the normal group and up-regulated in the tumor group (Figure 4E). At the same time, we conducted a paired difference analysis on the samples of CXCR4 and found that the level of CXCR4 expression was significantly different in the paracancer group and the tumor group ( $P < 0.05$ , Figure 4F). Finally, we further verified the CXCR4 expression in the Gene Expression Profiling Interactive Analysis (GEPIA, <http://gepia.cancer-pku.cn/>) database, and the results were consistent with the above results (Figure 4G).

#### **5. Analysis of CXCR4 gene**

According to the median value of CXCR4 gene expression level, GC patients were divided into high expression group and low expression group. The study found that the 5-year survival rate of the low expression group was higher than that of the high expression group (Figure 5A). Clinical studies of the CXCR4 gene showed that the expression of CXCR4 in GC patients is significantly different in age, grade, stage, T, and N (Figure 5B-H). Furthermore, CXCR4-related KEGG pathways were analyzed by GSEA software. GSEA analysis demonstrated that the CXCR4 gene was associated with several immune-associated signaling pathways, including intestinal immune network for IgA production (NES = 2.119,  $P < 0.001$ ), leukocyte transendothelial migration (NES = 2.188,  $P < 0.001$ ), natural killer cell mediated cytotoxicity (NES = 2.120,  $P < 0.001$ ), and T cell receptor signaling pathway (NES = 2.113,  $P < 0.001$ ) (Figure 5I, J).

#### **6. Correlation Between CXCR4 and Tumor Immune Cell Infiltration**

The CIBERSORT algorithm was employed to determine the degree of infiltration of immune cells in GC samples (Figure 6A). Moreover, different correlation patterns among the immune cells were found in TCGA cohorts (Figure 6B). As a result, T cells CD4 memory activated was negatively correlated with B cells naïve, T cells regulatory (Tregs), and T cells CD4+ (CD4+ T) memory resting, but positively correlated with Macrophages M1 and T cells CD8+ (CD8+ T). Also, the contents of immune cells varied among different immune groups (Figure 6C).

The expression level of CXCR4 was positively correlated with the infiltration degree of immune cells (Figure 6D). By analyzing the differences of 22 immune cells in the high expression group and low expression group of CXCR4, we found that CXCR4 gene expression was significantly correlated with B cells naïve, B cells memory, T cells gamma delta, Monocytes, and Macrophages M0 (Figure 6E). As shown in Figure F, B cells naïve, B cells memory, CD8+ T, T cells gamma delta, Mast cells activated, and Eosinophils infiltration were positively correlated with the high expression group of CXCR4, while Neutrophils, Macrophages M0, Mast cells activated, and Dendritic cells (DC) activated infiltration reached an inverse outcome.

## 7. The Prognostic Implication of CXCR4-related Immunomodulator in gastric Cancer

We identified 20 immunoinhibitors (ADORA2A, BTLA, CD160, CD244, CD274, CD96, CSF1R, CTLA4, HAVCR2, IDO1, IL10, KDR, LAG3, LGALS9, PDCD1, PDCD1LG2, PVRL2, TGFB1, TGFBR1, and TIGIT), 37 immunostimulators (CXCR4, ENTPDI, HHLA2, ICOS, ICOSLG, IL2RA, IL6, IL6R, KLRC1, KLRK1, LTA, PVR, TMEM173, TMIGD2, TNFRSF13B, TNFRSF13C, TNFRSF17, TNFRSF18, TNFRSF25, TNFRSF4, TNFRSF8, TNFRSF9, TNFSF13B, TNFSF14, TNFSF18, TNFSF4, and ULBP1) and 16 MHC molecules (MHC molecule B2M, HLA-A, HLA-B, HLA-C, HLA-DMA, HLA-DMB, HLA-DOA, HLA-DOB, HLA-DPA1, HLA-DPB1, HLA-DQAI, HLA-DQA2, HLA-DQBI, HLA-DRA, HLA-DRB1, and HLA-E) significantly associated with CXCR4 in GC (Figure 7A). The volcano plot showed the 10 top genes that were tightly correlated to these immunomodulators (Figure 7B).

To investigate the prognostic values of CXCR4-associated immunomodulators in GC, we entered these variables into univariate and multivariate Cox regression analysis. This method led to an optimal 2-gene prognostic signature in GC. And we constructed a 2-gene prognostic model. The Cox regression analysis and the biological functions of the genes are presented in Table 1. The risk scores were calculated by adding up the product of expression value and coefficient of each gene. The Kaplan-Meier survival curve elucidated that patients with low-risk scores had a higher 5-year survival rate than those with high risk (log-rank test,  $P < 0.001$ ) (Figure 7C). The area under the curve (AUC) value of the risk score was 0.598 (Figure 7D). The distribution of risk scores, survival statuses, and the risk genes expression profiles for GC was visualized in Figure 7E. Figure 7F, G showed the correlation between the risk score and the survival rate in TCGA-STAD in univariate and multivariate COX regression models. Moreover, univariate Cox regression demonstrated that the risk score was an independent predictor of prognosis in GC after adjusting for age, gender, stage, T, M, and N (HR = 2.119, 95% CI = 1.196–3.755,  $P = 0.010$ ).

Table 1

Gene	Full name of gene	Functions	Coefficient	Univariate analysis	
				HR (95% CI)	p-value
CD86	CD86 molecule	coreceptor activity; protein binding; signaling receptor activity; virus receptor activity	0.0437	1.06(1.00-1.12)	0.044
TNFSF18	TNF superfamily member 18	cytokine activity; identical protein binding; protein binding; signaling receptor binding; tumor necrosis factor receptor superfamily binding; tumor necrosis factor receptor superfamily binding	0.1559	1.22(1.02-.47)	0.033
Lasso Cox analysis					

Finally, we constructed a prognostic nomogram in GC to anticipate the individuals' survival probability by weighing risk score, stage, grade, T, N, M, age, and gender (Fig. 7H). We also used time-dependent ROC to evaluate the predictive discrimination of the nomogram (Fig. 7I). The AUC values of the 1-year, 3-year, and 5-year were 0.59, 0.58 and 0.54, respectively.

## Discussion

TME is a complex system involving multiple cells and cytokines, which has been reported to play an essential role in the treatment and prognosis of tumors and has become a research hotspot in immunotherapy and precision treatment of malignant tumors [25, 26]. Our results obtained by the ESTIMATE algorithm showed that the low score group of the stromal score has a higher 5-year survival rate than the high score group of the stromal score, which was consistent with a previous study of Zhou et al. [27], supporting the conclusions that the content of stromal cells in the GC microenvironment was related to the survival of patients. The correlation analyses of stromal and immune scores with clinical parameters of GC revealed that both high stromal and immune scores were related to poor tumor differentiation and severe local invasion and that neither was significantly related to lymph nodes and distant metastasis, indicative of the greater influence of TME on primary tumor cells than metastasis. Based on the hierarchical clustering algorithm, the samples were clustered into the Immunity High/Medium/Low groups. The results indicated that the Immunity High group had the highest infiltration degree of stromal and immune cells, and the lowest level of tumor purity. This finding was consistent with those of previous studies in which patients with higher immunological responses usually showed enrichment of stromal cells and immune cells in the TME [23]. Through functional enrichment analysis of 760 DEGs, we found that the DEGs were associated with immune function. In our study, all of the 26 genes related to prognosis were high-risk genes in GC, unfortunately, indicating poor prognosis.

The intersection of 30 PPI hub genes and 26 prognostic-related genes was taken to obtain the CXCR4 gene. CXCR4 can promote tumor cell growth, migration, and invasiveness [29, 30]. CXCR4 expression in various cancer was significantly correlated with lymph node and distant metastasis and worse overall survival [31–34], building a therapeutic rationale for CXCR4 targeting. CXCR4 has been experimentally confirmed to be associated with the pathogenesis or prognosis of GC or other malignancies [19, 35, 36]. Generally, high CXCR4 expression of solid tumors is related to poor prognosis. Our study reached the same conclusion and found that patients with low expression of CXCR4 had a better prognosis. CXCR4-related KEGG pathways included intestinal immune network for IgA production, leukocyte transendothelial migration, natural killer cell mediated, and T cell receptor signaling pathway. The results of the CIBERSORT algorithm in our study showed B cells naïve, B cells memory, CD8+ T cells gamma delta, Mast cells activated, and Eosinophils infiltration were positively correlated with the high expression group of CXCR4, while Neutrophils, Macrophages M0, Mast cells activated, and Dendritic cells (DCs) activated infiltration reached an inverse outcome. CD8+ T, also known as cytotoxic T cell (CTL), has the anti-tumor immune function and promotes tumor cell apoptosis, and has good clinical effects on various malignant tumors, including GC [37–39]. B cells are able to promote immune response and anti-tumor immune responses [40, 41], and are associated with a favorable prognosis for several cancer types [42,

43]. Tumor-associated macrophages (TAMs) promote tumor angiogenesis, maintain stem cells, and suppress immune responses [44]. The high infiltration of TAM promotes tumorigenesis and is correlated with poor overall survival in breast, gastric, oral, ovarian, bladder, and thyroid cancers [45]. DCs are the most potent APCs able to activate naive T cells and can induce immune memory responses in cancer [46, 47].

In vitro experiments confirmed that tyrosine kinase inhibitors imatinib and nilotinib could selectively increase the cell surface of CXCR4 on Natural killer (NK) cells and monocytes [48]. On a preclinical level, TN14003 and AMD3100, two anti-CXCR4 inhibitors, have anti-tumor activity against HER2 subtype of breast cancer [49]. In the test of the murine model of human pancreatic cancer, AMD3100 could not only successfully block CXCR4 signaling and promote T cell mobilization in vivo, but also showed higher anti-cancer activity when combined with an anti-PD-L1 monoclonal antibody [50–52], exhibiting similar promising preclinical results. It has been found that the introduction of oncolytic viruses equipped with CXCR4 antagonists can restore pathological signaling in a murine model of ovarian cancer, diminish metastatic spread and decrease regulatory T cell recruitment [53]. Moreover, NK cells co-expressed with a chimeric antigen receptor and chemokine receptor CXCR4 increased NK cell infiltration and enhanced tumor cell killing effect [54]. In particular, studies have found that the CXCR4-CXCL12 axis is involved in the development of B, T, and NK cells [55, 56]. In vitro, CXCL12-KDEL retention protein was used to block colon cancer cells, resulting in inhibition of CXCR4-mediated signaling and a significant reduction in the growth of metastatic cancer [57]. GC can also benefit from the inhibition of the CXCR4-CXCL12 axis [58].

## Conclusion

In this study, we found a close linkage between CXCR4 and the immunity of GC. The CXCR4 gene expression was associated with immune cell infiltration levels and immunomodulators. We established an immune gene model for GC using CXCR4-associated immunomodulators. The risk scores derived from the gene signatures were significantly associated with survival in GC. Subsequently, we constructed a nomogram for personalized prognosis prediction. And, we used time-dependent ROC to evaluate the predictive discrimination of the nomogram. Our results demonstrated that the risk scores derived from CXCR4-associated immunomodulators could distinguish risk groups defined by differential expression of a set of signature genes. Our findings may accelerate the development of verification signatures for the prognosis of GC.

In summary, our results suggest that CXCR4 may also play a role in the regulation of tumor immune microenvironment. The prognostic immune markers from CXCR4-associated immunomodulators can independently predict the overall survival of GC. Prospective studies are needed to verify the clinical application of biomarkers in personalized management of GC.

## Declarations

### Ethics approval and consent to participate

Not applicable.

### **Consent for publication**

Consent for publication in this magazine.

### **Availability of data and materials**

All data and materials are available.

### **Competing interests**

The authors have declared that no competing interest exists.

### **Funding**

This study was supported by National Natural Science Foundation of China [No.81673918], Pilot gastric cancer project of clinical cooperation of traditional Chinese and western medicine for major and difficult diseases, The Open Projects of the Discipline of Chinese Medicine of Nanjing University of Chinese Medicine Supported by the Subject of Academic priority discipline of Jiangsu Higher Education Institutions [No.ZYX03KF020], and National Administration of Traditional Chinese Medicine : 2019 Project of building evidence based practice capacity for TCM[No.2019XZZX-ZL003].

### **Authors' contributions**

Fang Wen conceived and designed the manuscript. Fang Wen wrote manuscript. Xiaona Lu and Wenjie Huang analyzed the data and generated the figures. Xiaoxue Chen and Shuai Ruan performed the literature search and collected data for the manuscript. Su Ping Gu, Yulang Wang, and Ye Li revised the images. Jiatong Liu and Shenlin Li revised the tables and checked the manuscript. Peng Shu directed the manuscript. All authors read and approved the final manuscript.

### **Acknowledgements**

Not applicable.

## **References**

1. Bray F, Ferlay J, Soerjomataram I, Siegel RL, Torre LA, Jemal A. Global cancer statistics 2018: GLOBOCAN estimates of incidence and mortality worldwide for 36 cancers in 185 countries. *CA Cancer J Clin*. 2018;68:394–424. <https://doi.org/10.3322/caac.21492>.
2. Verdecchia A, Francisci S, Brenner H, Gatta G, Micheli A, Mangone L, Kunkler I, EURO-CARE-4 Working Group. Recent cancer survival in Europe: a 2000-02 period analysis of EURO-CARE-4 data. *Lancet Oncol*. 2007;8:784–96. [https://doi.org/10.1016/S1470-2045\(07\)70246-2](https://doi.org/10.1016/S1470-2045(07)70246-2).
3. Ajani JA, Lee J, Sano T, Janjigian YY, Fan D, Song S. Gastric adenocarcinoma. *Nature Reviews Disease Primers*. 2017;3:1–19. <https://doi.org/10.1038/nrdp.2017.36>.
4. Chiurillo MA. Role of the Wnt/ $\beta$ -catenin pathway in gastric cancer: An in-depth literature review. *World J Exp Med*. 2015;5:84–102. <https://doi.org/10.5493/wjem.v5.i2.84>.
5. Jiang X, Wang J, Deng X, Xiong F, Ge J, Xiang B, Wu X, Ma J, Zhou M, Li X, Li Y, Li G, Xiong W, Guo C, Zeng Z. Role of the tumor microenvironment in PD-L1/PD-1-mediated tumor immune escape, *Mol Cancer*. 18 (2019). <https://doi.org/10.1186/s12943-018-0928-4>.

6. Ren Q, Zhu P, Zhang H, Ye T, Liu D, Gong Z, Xia X. Identification and validation of stromal-tumor microenvironment-based subtypes tightly associated with PD-1/PD-L1 immunotherapy and outcomes in patients with gastric cancer, *Cancer Cell Int* 20 (2020). <https://doi.org/10.1186/s12935-020-01173-3>.
7. Hanahan D, Weinberg RA. The hallmarks of cancer. *Cell*. 2000;100:57–70. [https://doi.org/10.1016/s0092-8674\(00\)81683-9](https://doi.org/10.1016/s0092-8674(00)81683-9).
8. Hanahan D, Coussens LM. Accessories to the crime: functions of cells recruited to the tumor microenvironment. *Cancer Cell*. 2012;21:309–22. <https://doi.org/10.1016/j.ccr.2012.02.022>.
9. Jia D, Li S, Li D, Xue H, Yang D, Liu Y. Mining TCGA database for genes of prognostic value in glioblastoma microenvironment, *Aging (Albany NY)*. 10 (2018) 592–605. <https://doi.org/10.18632/aging.101415>.
10. Remon J, Besse B. Immune checkpoint inhibitors in first-line therapy of advanced non-small cell lung cancer. *Curr Opin Oncol*. 2017;29:97–104. <https://doi.org/10.1097/CCO.0000000000000351>.
11. Liu X, Cho WC. Precision medicine in immune checkpoint blockade therapy for non-small cell lung cancer, *Clin Transl Med* 6 (2017). <https://doi.org/10.1186/s40169-017-0136-7>.
12. Hanahan D, Weinberg RA. Hallmarks of Cancer: The Next Generation. *Cell*. 2011;144:646–74. <https://doi.org/10.1016/j.cell.2011.02.013>.
13. Li B, Cui Y, Diehn M, Li R. Development and Validation of an Individualized Immune Prognostic Signature in Early-Stage Nonsquamous Non–Small Cell Lung Cancer. *JAMA Oncol*. 2017;3:1529–37. <https://doi.org/10.1001/jamaoncol.2017.1609>.
14. Liu X, Wu S, Yang Y, Zhao M, Zhu G, Hou Z. The prognostic landscape of tumor-infiltrating immune cell and immunomodulators in lung cancer. *Biomedicine Pharmacotherapy*. 2017;95:55–61. <https://doi.org/10.1016/j.biopha.2017.08.003>.
15. Chen B, Khodadoust MS, Liu CL, Newman AM, Alizadeh AA. Profiling Tumor Infiltrating Immune Cells with CIBERSORT. In: von Stechow L, editor. *Cancer Systems Biology: Methods and Protocols*. New York: Springer; 2018. pp. 243–59. [https://doi.org/10.1007/978-1-4939-7493-1\\_12](https://doi.org/10.1007/978-1-4939-7493-1_12).
16. Gentles AJ, Newman AM, Liu CL, Bratman SV, Feng W, Kim D, Nair VS, Xu Y, Khuong A, Hoang CD, Diehn M, West RB, Plevritis SK, Alizadeh AA. The prognostic landscape of genes and infiltrating immune cells across human cancers. *Nature Medicine*. 2015;21:938–45. <https://doi.org/10.1038/nm.3909>.
17. Yang X, Shi Y, Li M, Lu T, Xi J, Lin Z, Jiang W, Guo W, Zhan C, Wang Q. Identification and validation of an immune cell infiltrating score predicting survival in patients with lung adenocarcinoma. *Journal of Translational Medicine*. 2019;17:217. <https://doi.org/10.1186/s12967-019-1964-6>.
18. Benedicto A, Romayor I, Arteta B. CXCR4 receptor blockage reduces the contribution of tumor and stromal cells to the metastatic growth in the liver. *Oncol Rep*. 2018;39:2022–30. <https://doi.org/10.3892/or.2018.6254>.
19. Jiang Q, Sun Y, Liu X. CXCR4 as a prognostic biomarker in gastrointestinal cancer: a meta-analysis. *Biomarkers*. 2019;24:510–6. <https://doi.org/10.1080/1354750X.2019.1637941>.

20. Salgia R, Weaver RW, McCleod M, Stille JR, Yan SB, Roberson S, Polzer J, Flynt A, Raddad E, Peek VL, Wijayawardana SR, Um SL, Gross S, Connelly MC, Morano C, Repollet M, Sanders R, Baeten K, D'Haese D, Spigel DR. Prognostic and predictive value of circulating tumor cells and CXCR4 expression as biomarkers for a CXCR4 peptide antagonist in combination with carboplatin-etoposide in small cell lung cancer: exploratory analysis of a phase II study. *Invest New Drugs*. 2017;35:334–44. <https://doi.org/10.1007/s10637-017-0446-z>.
21. Chen IX, Chauhan VP, Posada J, Ng MR, Wu MW, Adstamongkonkul P, Huang P, Lindeman N, Langer R, Jain RK. Blocking CXCR4 alleviates desmoplasia, increases T-lymphocyte infiltration, and improves immunotherapy in metastatic breast cancer. *Proc Natl Acad Sci U S A*. 2019;116:4558–66. <https://doi.org/10.1073/pnas.1815515116>.
22. Liu Y, Ren C-C, Yang L, Xu Y-M, Chen Y-N. Role of CXCL12-CXCR4 axis in ovarian cancer metastasis and CXCL12-CXCR4 blockade with AMD3100 suppresses tumor cell migration and invasion in vitro. *J Cell Physiol*. 2019;234:3897–909. <https://doi.org/10.1002/jcp.27163>.
23. Heagerty PJ, Lumley T, Pepe MS. Time-dependent ROC curves for censored survival data and a diagnostic marker. *Biometrics*. 2000;56:337–44. <https://doi.org/10.1111/j.0006-341x.2000.00337.x>.
24. Iasonos A, Schrag D, Raj GV, Panageas KS. How to build and interpret a nomogram for cancer prognosis. *J Clin Oncol*. 2008;26:1364–70. <https://doi.org/10.1200/JCO.2007.12.9791>.
25. Straussman R, Morikawa T, Shee K, Barzily-Rokni M, Qian ZR, Du J, Davis A, Mongare MM, Gould J, Frederick DT, Cooper ZA, Chapman PB, Solit DB, Ribas A, Lo RS, Flaherty KT, Ogino S, Wargo JA, Golub TR. Tumor microenvironment induces innate RAF-inhibitor resistance through HGF secretion. *Nature*. 2012;487:500–4. <https://doi.org/10.1038/nature11183>.
26. Muro K, Van Cutsem E, Narita Y, Pentheroudakis G, Baba E, Li J, Ryu M-H, Zamanian WIW, Yong W-P, Yeh K-H, Kato K, Lu Z, Cho BC, Nor IM, Ng M, Chen L-T, Nakajima TE, Shitara K, Kawakami H, Tsushima T, Yoshino T, Lordick F, Martinelli E, Smyth EC, Arnold D, Minami H, Tabernero J, Douillard J-Y. Pan-Asian adapted ESMO Clinical Practice Guidelines for the management of patients with metastatic gastric cancer: a JSMO-ESMO initiative endorsed by CSCO, KSMO, MOS, SSO and TOS, *Ann Oncol*. 30 (2019) 19–33. <https://doi.org/10.1093/annonc/mdy502>.
27. Zhou L, Huang W, Yu H-F, Feng Y-J, Teng X. Exploring TCGA database for identification of potential prognostic genes in stomach adenocarcinoma, *Cancer Cell Int* 20 (2020). <https://doi.org/10.1186/s12935-020-01351-3>.
28. He Y, Jiang Z, Chen C, Wang X. Classification of triple-negative breast cancers based on Immunogenomic profiling. *J Exp Clin Cancer Res*. 2018;37:327. <https://doi.org/10.1186/s13046-018-1002-1>.
29. Müller A, Homey B, Soto H, Ge N, Catron D, Buchanan ME, McClanahan T, Murphy E, Yuan W, Wagner SN, Barrera JL, Mohar A, Verástegui E, Zlotnik A. Involvement of chemokine receptors in breast cancer metastasis. *Nature*. 2001;410:50–6. <https://doi.org/10.1038/35065016>.
30. Scotton CJ, Wilson JL, Scott K, Stamp G, Wilbanks GD, Fricker S, Bridger G, Balkwill FR. Multiple actions of the chemokine CXCL12 on epithelial tumor cells in human ovarian cancer. *Cancer Res*.

2002;62:5930–8.

31. Zhang Z, Ni C, Chen W, Wu P, Wang Z, Yin J, Huang J, Qiu F. Expression of CXCR4 and breast cancer prognosis: a systematic review and meta-analysis. *BMC Cancer*. 2014;14:49. <https://doi.org/10.1186/1471-2407-14-49>.
32. Sun Y-X, Wang J, Shelburne CE, Lopatin DE, Chinnaiyan AM, Rubin MA, Pienta KJ, Taichman RS. Expression of CXCR4 and CXCL12 (SDF-1) in human prostate cancers (PCa) in vivo. *J Cell Biochem*. 2003;89:462–73. <https://doi.org/10.1002/jcb.10522>.
33. Scala S, Ottaiano A, Ascierto PA, Cavalli M, Simeone E, Giuliano P, Napolitano M, Franco R, Botti G, Castello G. Expression of CXCR4 predicts poor prognosis in patients with malignant melanoma. *Clin Cancer Res*. 2005;11:1835–41. <https://doi.org/10.1158/1078-0432.CCR-04-1887>.
34. Choi YH, Burdick MD, Strieter BA, Mehrad B, Strieter RM. CXCR4, but not CXCR7, discriminates metastatic behavior in non-small cell lung cancer cells. *Mol Cancer Res*. 2014;12:38–47. <https://doi.org/10.1158/1541-7786.MCR-12-0334>.
35. Xu C, Zheng L, Li D, Chen G, Gu J, Chen J, Yao Q. CXCR4 overexpression is correlated with poor prognosis in colorectal cancer. *Life Sci*. 2018;208:333–40. <https://doi.org/10.1016/j.lfs.2018.04.050>.
36. Sakitani K, Hayakawa Y, Deng H, Ariyama H, Kinoshita H, Konishi M, Ono S, Suzuki N, Ihara S, Niu Z, Kim W, Tanaka T, Liu H, Chen X, Taylor Y, Fox JG, Konieczny SF, Onodera H, Sepulveda AR, Asfaha S, Hirata Y, Worthley DL, Koike K, Wang TC. CXCR4-expressing Mist1 + progenitors in the gastric antrum contribute to gastric cancer development. *Oncotarget*. 2017;8:111012–25. <https://doi.org/10.18632/oncotarget.22451>.
37. Najafi M, Goradel NH, Farhood B, Salehi E, Solhjoo S, Toolee H, Kharazinejad E, Mortezaee K. Tumor microenvironment: Interactions and therapy. *J Cell Physiol*. 2019;234:5700–21. <https://doi.org/10.1002/jcp.27425>.
38. Fu C, Jiang A. Dendritic Cells and CD8 T Cell Immunity in Tumor Microenvironment, *Front Immunol*. 9 (2018). <https://doi.org/10.3389/fimmu.2018.03059>.
39. Kim K-J, Lee KS, Cho HJ, Kim YH, Yang HK, Kim WH, Kang GH. Prognostic implications of tumor-infiltrating FoxP3 + regulatory T cells and CD8 + cytotoxic T cells in microsatellite-unstable gastric cancers. *Hum Pathol*. 2014;45:285–93. <https://doi.org/10.1016/j.humpath.2013.09.004>.
40. Fremd C, Schuetz F, Sohn C, Beckhove P, Domschke C. B cell-regulated immune responses in tumor models and cancer patients, *Oncolimmunology*. 2 (2013) e25443. <https://doi.org/10.4161/onci.25443>.
41. Nelson BH, Cells CD20 + B. The Other Tumor-Infiltrating Lymphocytes. *The Journal of Immunology*. 2010;185:4977–82. <https://doi.org/10.4049/jimmunol.1001323>.
42. Schmidt M, Böhm D, von Törne C, Steiner E, Puhl A, Pilch H, Lehr H-A, Hengstler JG, Kölbl H, Gehrmann M. The Humoral Immune System Has a Key Prognostic Impact in Node-Negative Breast Cancer. *Cancer Res*. 2008;68:5405–13. <https://doi.org/10.1158/0008-5472.CAN-07-5206>.
43. Iglesia MD, Vincent BG, Parker JS, Hoadley KA, Carey LA, Perou CM, Serody JS. Prognostic B-cell Signatures Using mRNA-Seq in Patients with Subtype-Specific Breast and Ovarian Cancer. *Clin*

- Cancer Res. 2014;20:3818–29. <https://doi.org/10.1158/1078-0432.CCR-13-3368>.
44. Ruffell B, Coussens LM. Macrophages and therapeutic resistance in cancer. *Cancer Cell*. 2015;27:462–72. <https://doi.org/10.1016/j.ccell.2015.02.015>.
  45. Baghdadi M, Wada H, Nakanishi S, Abe H, Han N, Putra WE, Endo D, Watari H, Sakuragi N, Hida Y, Kaga K, Miyagi Y, Yokose T, Takano A, Daigo Y, Seino K. Chemotherapy-Induced IL34 Enhances Immunosuppression by Tumor-Associated Macrophages and Mediates Survival of Chemoresistant Lung Cancer Cells. *Cancer Res*. 2016;76:6030–42. <https://doi.org/10.1158/0008-5472.CAN-16-1170>.
  46. Rowshanravan B, Halliday N, Sansom DM. CTLA-4: a moving target in immunotherapy. *Blood*. 2018;131:58–67. <https://doi.org/10.1182/blood-2017-06-741033>.
  47. Kreutz M, Tacke PJ, Figdor CG. Targeting dendritic cells—why bother? *Blood*. 2013;121:2836–44. <https://doi.org/10.1182/blood-2012-09-452078>.
  48. Bellora F, Dondero A, Corrias MV, Casu B, Regis S, Caliendo F, Moretta A, Cazzola M, Elena C, Vinti L, Locatelli F, Bottino C, Castriconi R. Imatinib and Nilotinib Off-Target Effects on Human NK Cells, Monocytes, and M2 Macrophages. *J Immunol*. 2017;199:1516–25. <https://doi.org/10.4049/jimmunol.1601695>.
  49. Lefort S, Thuleau A, Kieffer Y, Sirven P, Bieche I, Marangoni E, Vincent-Salomon A, Mehta-Grigoriou F. CXCR4 inhibitors could benefit to HER2 but not to triple-negative breast cancer patients. *Oncogene*. 2017;36:1211–22. <https://doi.org/10.1038/onc.2016.284>.
  50. Feig C, Jones JO, Kraman M, Wells RJB, Deonarine A, Chan DS, Connell CM, Roberts EW, Zhao Q, Caballero OL, Teichmann SA, Janowitz T, Jodrell DI, Tuveson DA, Fearon DT. Targeting CXCL12 from FAP-expressing carcinoma-associated fibroblasts synergizes with anti-PD-L1 immunotherapy in pancreatic cancer. *Proc Natl Acad Sci U S A*. 2013;110:20212–7. <https://doi.org/10.1073/pnas.1320318110>.
  51. Brahmer JR, Tykodi SS, Chow LQM, Hwu W-J, Topalian SL, Hwu P, Drake CG, Camacho LH, Kauh J, Odunsi K, Pitot HC, Hamid O, Bhatia S, Martins R, Eaton K, Chen S, Salay TM, Alaparthy S, Grosso JF, Korman AJ, Parker SM, Agrawal S, Goldberg SM, Pardoll DM, Gupta A, Wigginton JM. Safety and Activity of Anti-PD-L1 Antibody in Patients with Advanced Cancer. *N Engl J Med*. 2012;366:2455–65. <https://doi.org/10.1056/NEJMoa1200694>.
  52. Li J-K, Yu L, Shen Y, Zhou L-S, Wang Y-C, Zhang J-H. Inhibition of CXCR4 activity with AMD3100 decreases invasion of human colorectal cancer cells in vitro. *World J Gastroenterol*. 2008;14:2308–13. <https://doi.org/10.3748/wjg.14.2308>.
  53. Gil M, Komorowski MP, Seshadri M, Rokita H, McGray AJR, Opyrchal M, Odunsi KO, Kozbor D. CXCL12/CXCR4 Blockade by Oncolytic Virotherapy Inhibits Ovarian Cancer Growth by Decreasing Immunosuppression and Targeting Cancer Initiating Cells. *J Immunol*. 2014;193:5327–37. <https://doi.org/10.4049/jimmunol.1400201>.
  54. Müller N, Michen S, Tietze S, Töpfer K, Schulte A, Lamszus K, Schmitz M, Schackert G, Pastan I, Temme A. Engineering NK cells modified with an EGFRvIII-specific chimeric antigen receptor to

- overexpress CXCR4 improves immunotherapy of CXCL12/SDF-1 $\alpha$ -secreting glioblastoma. *J Immunother.* 2015;38:197–210. <https://doi.org/10.1097/CJI.0000000000000082>.
55. Sugiyama T, Kohara H, Noda M, Nagasawa T. Maintenance of the hematopoietic stem cell pool by CXCL12-CXCR4 chemokine signaling in bone marrow stromal cell niches. *Immunity.* 2006;25:977–88. <https://doi.org/10.1016/j.immuni.2006.10.016>.
56. Noda M, Omatsu Y, Sugiyama T, Oishi S, Fujii N, Nagasawa T. CXCL12-CXCR4 chemokine signaling is essential for NK-cell development in adult mice. *Blood.* 2011;117:451–8. <https://doi.org/10.1182/blood-2010-04-277897>.
57. Zeelenberg IS, Ruuls-Van Stalle L, Roos E. The chemokine receptor CXCR4 is required for outgrowth of colon carcinoma micrometastases. *Cancer Res.* 2003;63:3833–9.
58. Xiang Z, Zhou Z-J, Xia G-K, Zhang X-H, Wei Z-W, Zhu J-T, Yu J, Chen W, He Y, Schwarz RE, Brekken RA, Awasthi N, Zhang C-H. A positive crosstalk between CXCR4 and CXCR2 promotes gastric cancer metastasis. *Oncogene.* 2017;36:5122–33. <https://doi.org/10.1038/onc.2017.108>.

## Figures

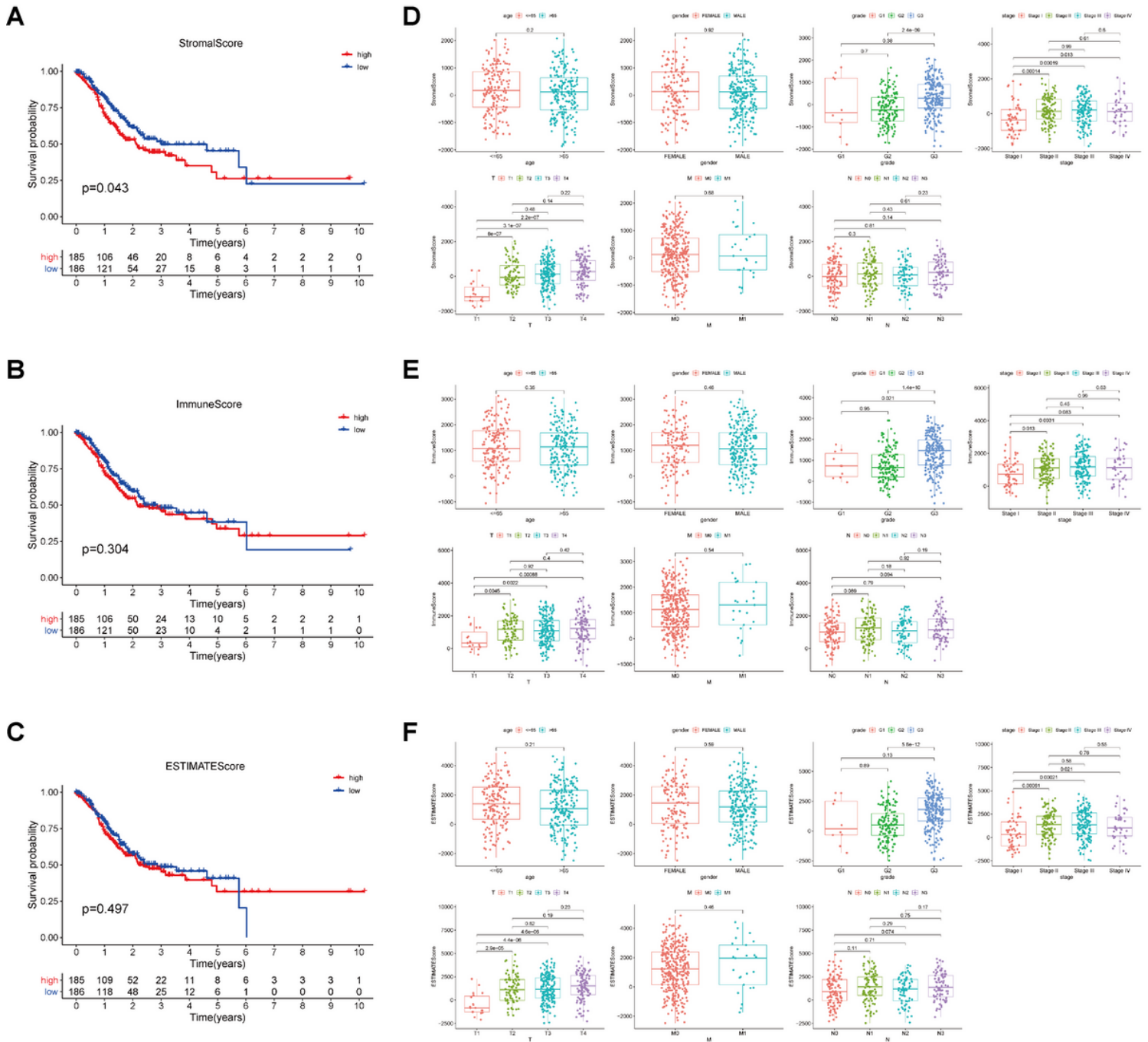


**Figure 1**

The potential relationship between the stromal/immune/estimate scores and the overall survival and clinical parameters of the samples. (A, B, C) The Kaplan–Meier survival curve showed that the correlation between the high and low score groups and 5-year survival rate. (D, E, F) The box plot indicated that correlation between the clinical parameters and the score levels.

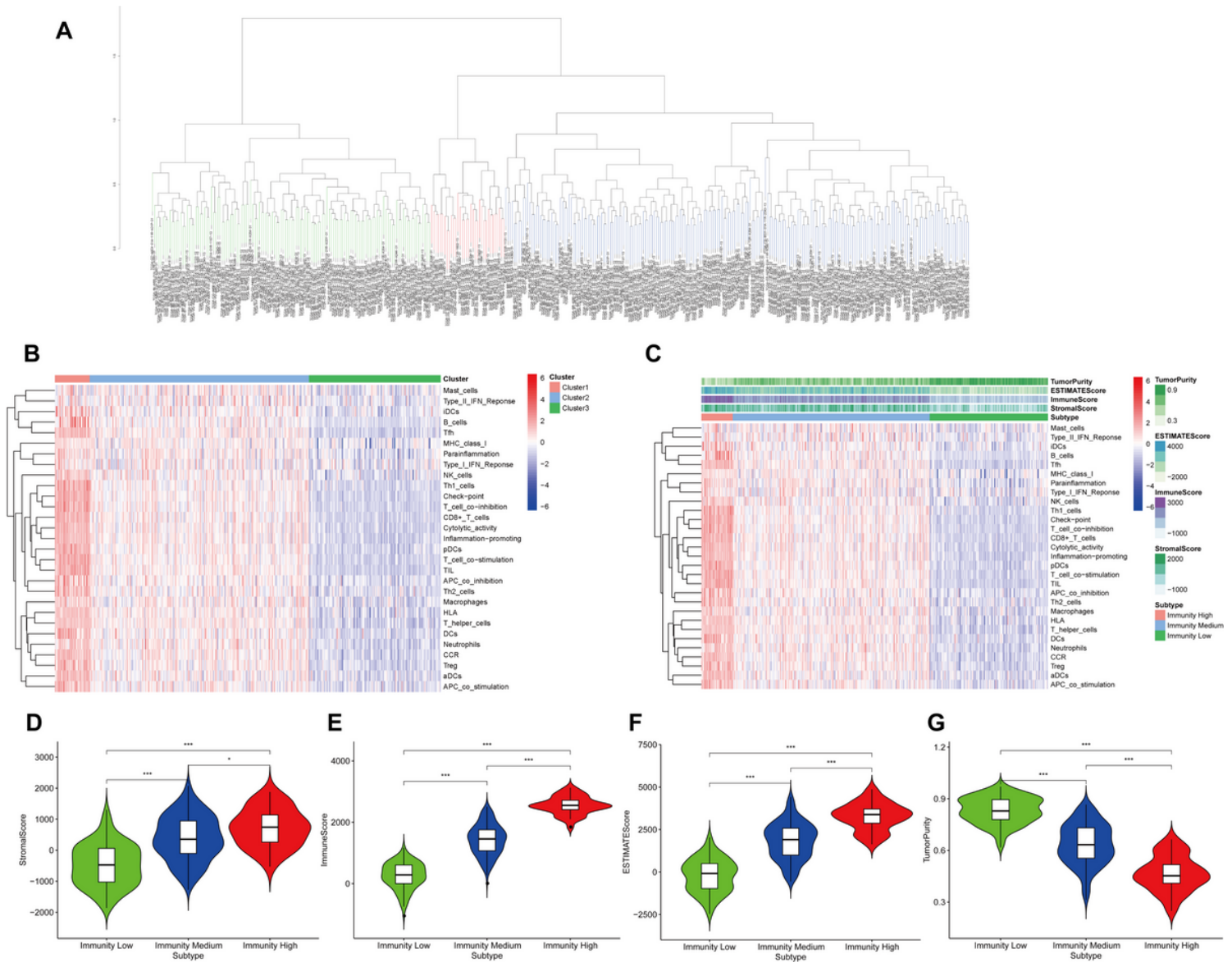


**Figure 2**

The tumor microenvironment and immunophenotypes of GC patients. (A) The samples were clustered into three categories by the hierarchical clustering algorithm. (B) The immune characteristics of Cluster 1, Cluster 2 and Cluster 3 were compared. (C) Landscape of the tumor microenvironment and immunophenotypes in the Immunity High/Medium/ Low groups by the tSNE algorithm and hierarchical clustering analysis. (D) Distribution of StromaScore in the Immunity High/Medium/ Low groups. (E) Distribution of ImmuneScore in the Immunity High/Medium/ Low groups. (F) Distribution of EstimateScore in the Immunity High/Medium/ Low groups. (G) Distribution of TumorPurity in the Immunity High/Medium/ Low groups.

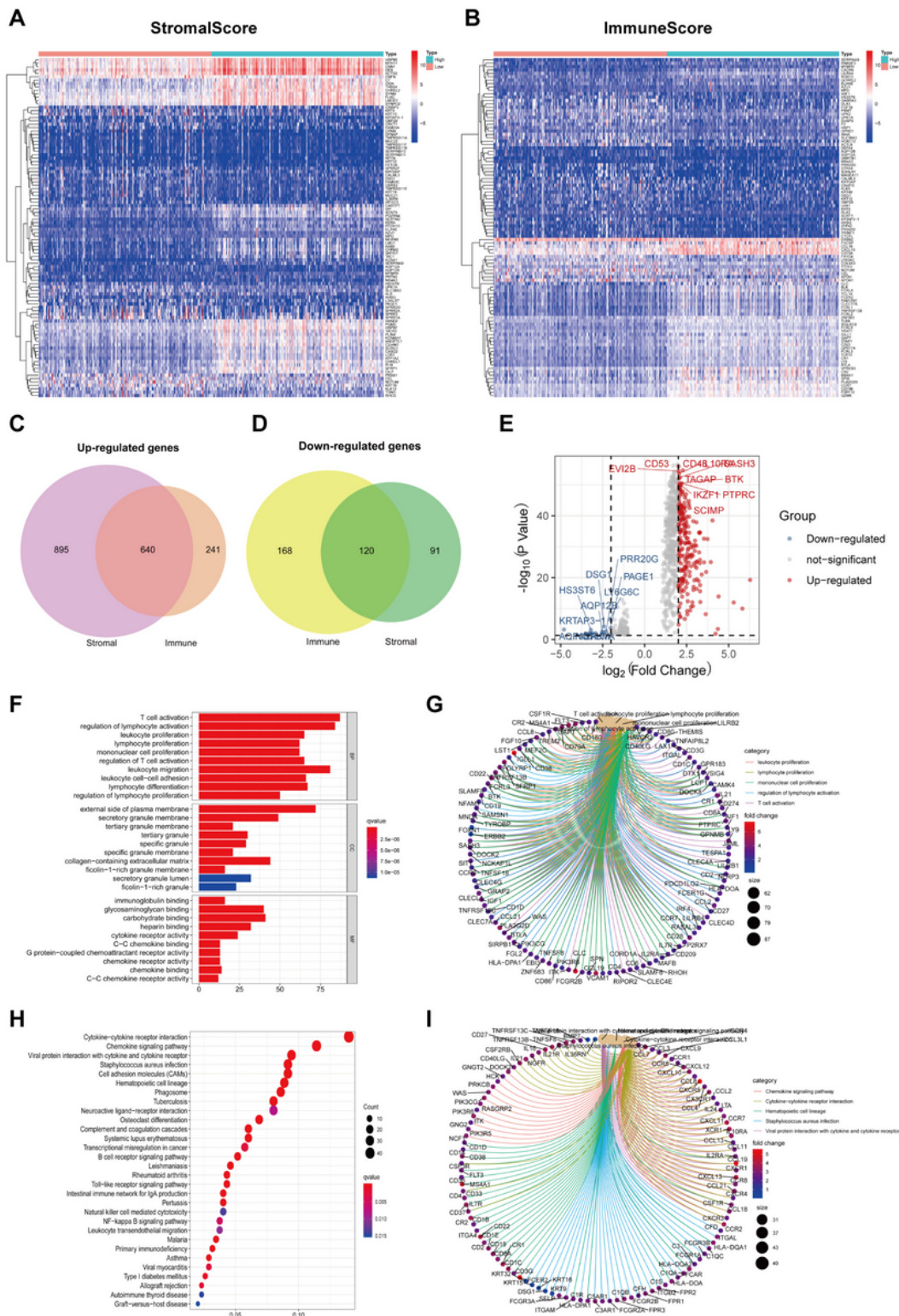


**Figure 3**

Identification and functional enrichment analysis of differentially expressed genes in GC patients. (A) The heat map of the differential genes with stromal scores of high score group and low score group ( $|\log_{2}FC| > 1$ ,  $FDR < 0.05$ ). (B) The heat map of the differential genes with immune scores of high score group and low score group ( $|\log_{2}FC| > 1$ ,  $FDR < 0.05$ ). (C) Venn diagram revealed the identical up-regulated differentially expressed genes between the stromal and immune cell groups. (D) Venn diagram revealed

the identical down-regulated differentially expressed genes between the stromal and immune cell groups. (E) The volcano plot showed the top 10 up-regulated genes and the top 10 down-regulated genes. (F, G) Top 10 GO terms from functional enrichment analysis of differentially expressed genes. (H, I) Top 30 KEGG pathway analysis of differentially expressed genes.

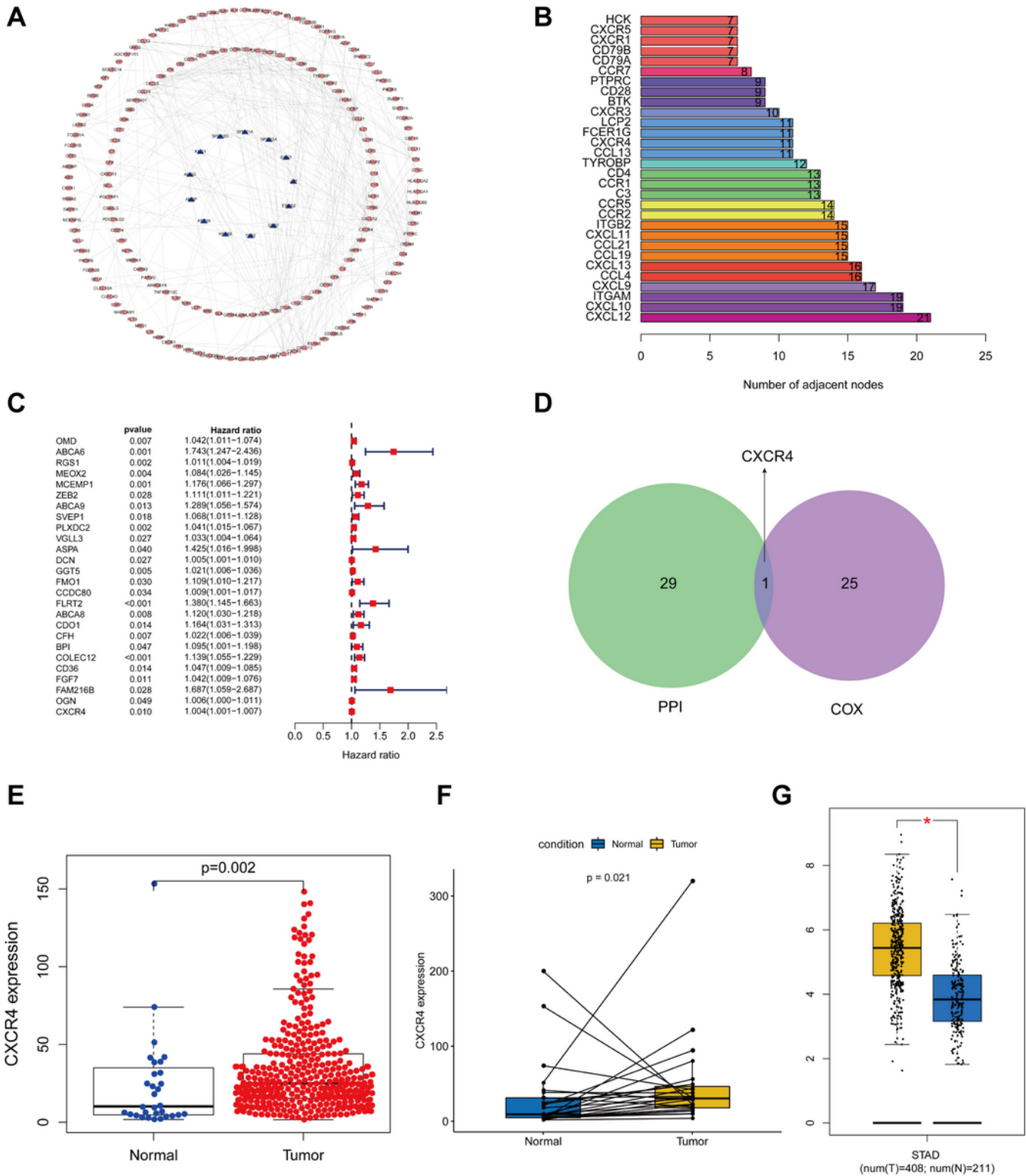
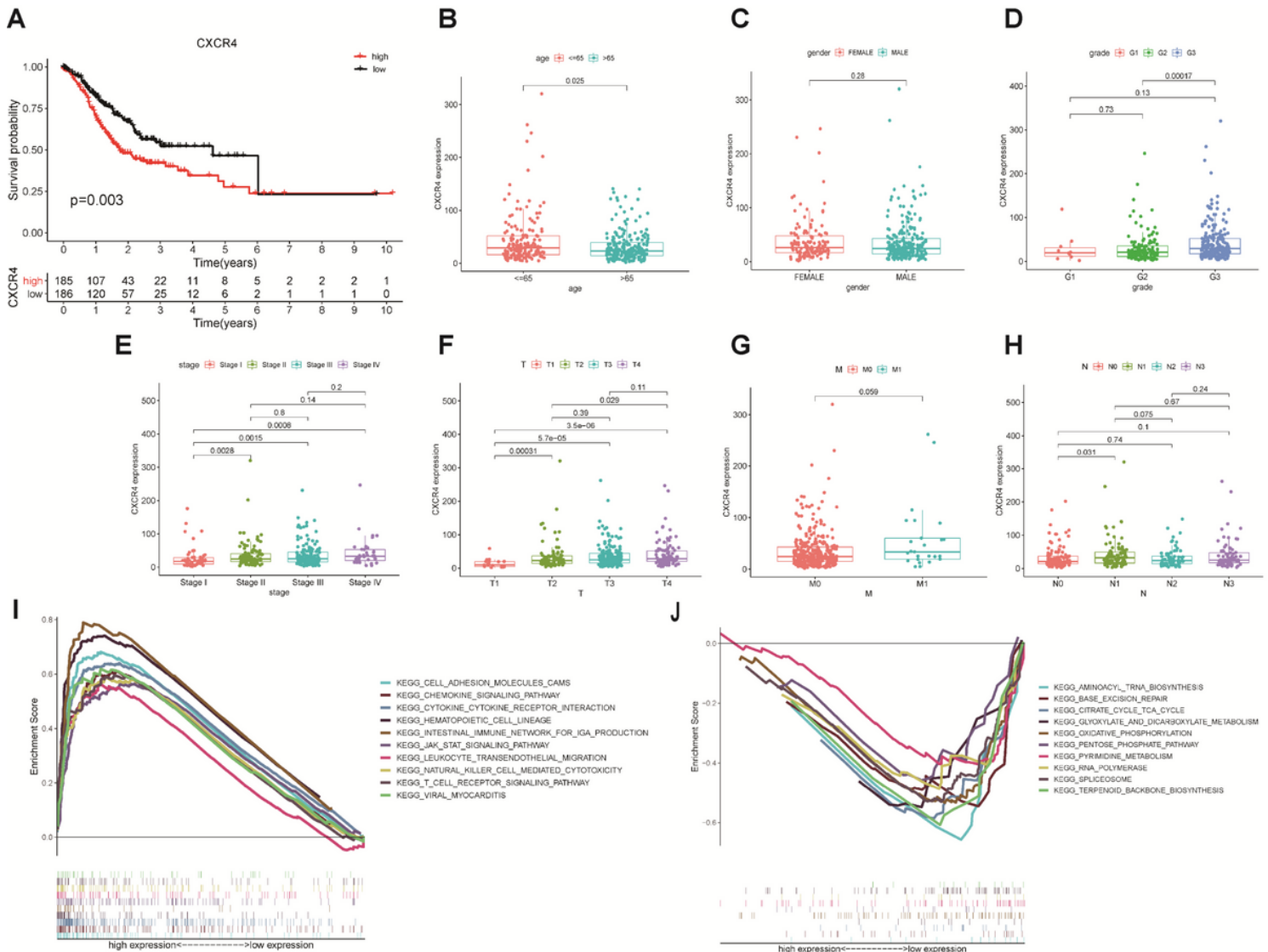


Figure 4

Identification and verification of CXCR4 gene. (A) The PPI network of genes with prognostic value. (B) The top 30 hub genes extracted from the PPI network. (C) The univariate COX analysis of 760 differentially expressed genes. (D) Identification of the hub prognostic gene. (E-G) verification of the hub prognostic gene. (E-G) verification of the hub prognostic gene.



**Figure 5**

Clinical analysis of CXCR4 gene. (A) Survival analysis of CXCR4 gene at different expression levels. (B-H) The expression level of CXCR4 gene in different clinical parameters. (I-J) Dissection of CXCR4-associated KEGG pathways by Gene Set Enrichment Analysis

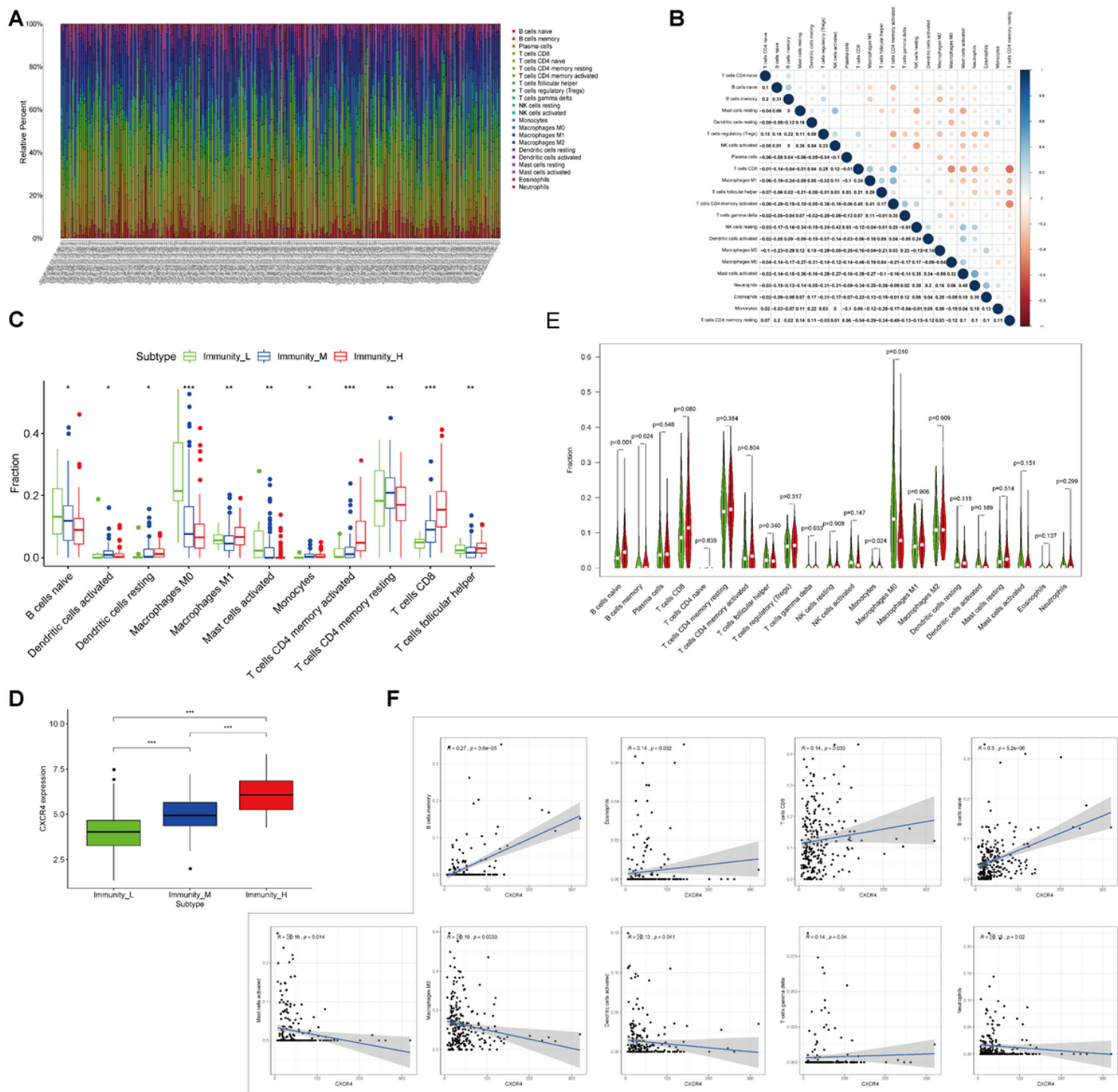


**Figure 6**

Relationship between CXCR4 and tumor immune cell infiltration. (A) Landscape of immune cell infiltration in TCGA-STAD samples determined by the CIBERSORT algorithm. (B) Different correlation patterns among 26 immune cell subsets in TCGA-STAD cohorts. (C) The content of immune cells was significantly different among different immunity groups. (D) The boxplot showed that the expression level of CXCR4 was positively correlated with the infiltration degree of immune cells. (E) Violin plots showed the differences in the immune cell distribution at high expression (red) and low expression (green) of CXCR4. (F) Correlation analysis of CXCR4 and immune cell infiltration.



clinical indices. (E) Distribution of risk scores, along with survival statuses, and gene expression profiles for GC. (F, G) Univariate and multivariate Cox regression analyses of the risk score in GC regarding overall survival. (H) Nomogram constructed in conjunction with the risk genes and clinical characterization. (I) Time-dependent ROC curve of the nomogram shows the ROC curve and AUC for 1-, 3-, and 5-year survival, respectively.